

Evidence for impacts on surface-level air quality in the Northeastern U.S. from long-distance transport of smoke from North American fires during LISTOS 2018

Haley M. Rogers¹, Jenna C. Ditto¹, Drew R. Gentner^{1,2}

¹ Department of Chemical and Environmental Engineering, Yale University, New Haven, CT, 06511, USA

² SEARCH (Solutions for Energy, Air, Climate and Health) Center, Yale University, New Haven, CT, USA.

Correspondence to: Drew R. Gentner (drew.gentner@yale.edu)

Abstract. Biomass burning is a large source of uncontrolled air pollutants, including particulate matter (i.e. PM_{2.5}), black carbon (BC), volatile organic compounds (VOCs), and carbon monoxide (CO), which have significant effects on air quality, human health, and climate. Measurements of PM_{2.5}, BC, and CO made at the Yale Coastal Field Station in Guilford, CT and five other sites in the metropolitan New York City (NYC) area indicate long-distance transport of pollutants from wildfires and other biomass burning to surface-level sites in the region. Here, we examine two such events occurring on August 16th-17th and 27th-29th, 2018. In addition to regionally-consistent enhancements in the surface concentrations of gases and particulates associated with biomass burning, satellite imagery confirms the presence of smoke plumes in the NYC-Connecticut region during these events. Backward-trajectory modeling indicates that air masses arriving at surface-level sites in coastal Connecticut on August 16th-17th passed over the west coast of Canada, near multiple large wildfires. In contrast, air parcels arriving on August 27th-29th passed over active fires in the southeastern United States. The results of this study demonstrate that biomass burning events throughout the U.S. and Canada (at times more than 4000 km away), which are increasing in frequency, impact surface-level air quality beyond regional scales, including in NYC and the northeastern U.S.

Keywords: LISTOS (Long Island Sound Tropospheric Ozone Study), biomass burning, wildfires, urban air quality

25 **1 Introduction**

26 Biomass burning, which occurs on a large scale during wildfires and some controlled burns, is a major source of air
27 pollutants that impact air quality, human health, and climate (Lewis et al., 2008; Liu et al., 2015; Reid et al., 2016;
28 Urbanski et al., 2008). During these events, gases such as carbon monoxide (CO), carbon dioxide (CO₂), methane
29 (CH₄), nitrous oxide (N₂O), nitrogen oxides (NO_x), and gas-phase organic compounds (including volatile organic
30 compounds (VOCs)) are directly released into the atmosphere (Akagi et al., 2011; Urbanski et al., 2008; Vicente et
31 al., 2013; Yokelson et al., 2013). Biomass burning produces particulate matter (PM), including black carbon (BC) and
32 other primary organic aerosol (POA) in the PM_{2.5} size range (i.e. particles with a diameter $\leq 2.5 \mu\text{m}$) (Akagi et al.,
33 2011; Urbanski et al., 2008). Biomass burning is also a source of reactive precursors to the production of secondary
34 compounds, such as ozone (O₃) and secondary organic aerosol (SOA) (Urbanski et al., 2008; Ward and Hardy, 1991).
35 The chemical composition of PM resulting from biomass burning depends on many factors, such as the type of fuel
36 and combustion conditions (Calvo et al., 2013). In addition to the environmental impacts of biomass burning
37 emissions, elevated PM_{2.5} concentrations have been associated with respiratory and cardiovascular disease, and higher
38 mortality rates (Brook et al., 2004; Dockery et al., 1993; Reid et al., 2016).

39
40 The pollutants emitted from biomass burning events affect not only local air quality, but can be transported over long
41 distances (Barnaba et al., 2011; Burgos et al., 2018; Forster et al., 2001; Martin et al., 2006; Niemi et al., 2005; Stohl
42 et al., 2003). Colarco et al. (2004) used satellite and other remote-sensing tools, combined with backward-trajectory
43 and 3-D models, to confirm the presence of pollution from July 2002 wildfire smoke that originated in Quebec, Canada
44 and was transported and detected at surface-level in Washington, D.C. Similar studies have described the long-range
45 transport of wildfire smoke from Canadian wildfires to Maryland (Dreessen et al., 2016), Siberian wildfires to British
46 Columbia (Cottle et al., 2014), as well as examples in Europe and Asia (Diapouli et al., 2014; Jung et al., 2016). Over
47 the course of this long-distance transport, the gas- and aerosol-phase compounds undergo aging and dilution. Organic
48 gases and aerosols are transformed chemically by photo-oxidation, interaction with atmospheric oxidants, and reaction
49 with other atmospheric compounds (Cubison et al., 2011; Hennigan et al., 2011). While more reactive components
50 will age more quickly, this study focused on tracers which are less likely to react over our transport timescales. For
51 example, BC is primarily removed via particle deposition to the Earth's surface, which is largely dependent on height
52 above ground level. Mixing of aloft plumes from the free troposphere is variable and can range from 1 week to 1

53 month with altitude, vertical transport conditions, and weather (Jacob, 1999), and PM_{2.5} losses due to physical
54 processes will follow similar timescales. Losses of these tracers is possible depending on timescales and weather
55 conditions (e.g. wet deposition) during long-distance transport. However, they are generally long-lived in the free
56 troposphere and many previous studies have used BC, CO, and/or PM_{2.5} as indicators of long-distance transport of
57 biomass burning smoke (Burgos et al., 2018; Cottle et al., 2014; Diapouli et al., 2014; Dreessen et al., 2016; Forster
58 et al., 2001; Martin et al., 2006; Niemi et al., 2005).

59
60 The impacts of wildfire smoke, both regionally and at long distances, will become increasingly important in the
61 coming years, with the number and severity of wildfires predicted to increase with climate change. Barbero et al.
62 (2015) used 17 global climate models to evaluate the effect of anthropogenic climate change on large-scale wildfires
63 in the U.S., and found that the likelihood of forest fires will increase across most historically fire-prone regions, likely
64 due to an earlier onset of summer and extended summer season. Abatzoglou and Williams (2016) similarly found that
65 wildfires are likely to increase in the coming years due to climate change impacts such as increased temperature and
66 decreased atmospheric water vapor pressure. As the risks of climate change and its relation to wildfires are realized,
67 it is increasingly important to understand the environmental and health effects that may be associated, including long-
68 distance transport.

69
70 The NYC metropolitan area (including parts of Connecticut and New Jersey) is home to approximately 20.3 million
71 people (U.S. Census Bureau, 2017) and has historically struggled with attainment to air quality standards. The
72 objective of this work is to evaluate the influence of North American biomass burning events on air quality in NYC
73 and the Northeast U.S. using measurements from the Yale Coastal Field Station (YCFS) in Guilford, Connecticut (on
74 the Long Island Sound) and other sites in the metropolitan NYC area, combined with satellite imagery and air parcel
75 backward-trajectory modeling. We focus on observations of two multi-day air pollution events during the month of
76 August 2018 during the LISTOS (Long Island Sound Tropospheric Ozone Study) 2018 field campaign, both of which
77 coincided with NYC air quality advisory period for ozone on August 16th, 28th, and 29th (New York Department of
78 Environmental Conservation, 2018).

79 **2 Materials and Methods**

80 We perform a multi-platform-based analysis to determine whether specific regional air pollution events occurring in
81 coastal Connecticut and the NYC area can be attributed to long-distance transport of emissions from wildfires and
82 other biomass burning. This analysis combines results from pollutant measurements taken at the YCFS and other
83 regional sites, satellite imagery (NOAA Smoke Maps), and the NOAA HYSPLIT backward-trajectory model. Each
84 of these techniques provides some evidence of the long-distance transport of wildfire pollutants, and we combine these
85 methods to evaluate potential sources and transport times.

86 **2.1 Yale Coastal Field Station Air Quality Measurements**

87 Ambient surface-level measurements were collected at the YCFS, located on the Long Island Sound in Guilford, CT
88 (41.2583°N, 72.7312°W) using reference instrumentation for PM_{2.5}, BC, and CO at 1 hour resolution for PM_{2.5}, 1
89 minute for BC, and 1 second for CO (BC and CO then averaged to 1 hour intervals). An AE33 Aethalometer (Magee
90 Scientific) was used to measure BC; a BAM-1020 (Met One) was used to measure PM_{2.5}; and a 48i CO analyzer
91 (Thermo Fisher) was used to measure CO. All instrument flow rates were calibrated, relevant zeroing procedures were
92 performed for the BC and PM_{2.5} measurements, and the CO instrument zero and span concentrations were calibrated
93 (using house-generated zero air and a CO standard from AirGas: ±5% standard 10 ppm CO in nitrogen diluted with
94 AliCat mass flow controllers). We corrected for CO calibration drift when necessary by adjusting the baseline to
95 regional background levels. Inlets for each of these instruments were positioned ~5 m from the water on a small tower
96 2.5-3 m above the ground, facing south (i.e. towards the Long Island Sound) with direct inflow from the water during
97 southerly onshore winds. Particulate inlets used PM_{2.5} cyclones and metal tubing (BC: copper; PM_{2.5}: stainless steel).
98 The CO inlet was constructed of FEP tubing (¼" OD) and PM was removed at the inlet using a PTFE filter (Tisch)
99 and PTFE filter holder. The YCFS is strategically positioned to minimize local urban influence from Connecticut
100 while also being in the NYC metro area. Thus, it serves as a regional background site with less local influence than
101 more urbanized stations.



102 **Figure 1: Location of air quality monitoring sites used for PM_{2.5}, BC, and CO measurements. Panel A shows all six sites,**
 103 **while panel B shows a close-up of the five sites directly on the Long Island Sound.**

104 These YCFS measurements were compared to data from other field sites (for the pollutants available) in the region
 105 (Figure 1), including EPA-related sites in New Haven, CT (Site 09-009-0027), Bridgeport, CT (Site 09-001-0010),
 106 Fort Griswold Park, CT (Site 09-011-0124), and Queens, NY (Site 36-081-0124), as well as data from the New York
 107 Department of Environmental Conservation’s rural site in Pinnacle State Park, NY. Sites were selected for regional
 108 proximity to the YCFS as well as data availability.

109 2.2 Satellite Imagery of Smoke Plumes

110 The NOAA Hazard Mapping System (HMS) generated Smoke Maps (NOAA, 2018) once a day based on satellite
 111 imagery of the spatial distribution of visible smoke plumes across North America. The data were downloaded from

112 the NOAA smoke products website and mapped via Google MyMaps. While these maps do not provide vertical
113 resolution on the distribution of the smoke plumes, they provide information on the horizontal distribution and density
114 of the smoke plumes in the region.

115 **2.3 NOAA HYSPLIT Air Parcel Backward-Trajectory Modeling**

116 The NOAA Hybrid Single Particle Lagrangian Integrated Trajectory (HYSPLIT) online software (Stein et al., 2015)
117 was used to run backward-trajectory models of air parcels arriving at the YCFS during the two periods of elevated
118 PM_{2.5}, BC, and CO. The HYSPLIT model used archived meteorological data to trace the transport of an air parcel
119 both vertically and horizontally through the atmosphere. The backward-trajectory model was run using GDAS1.0
120 meteorological data over a 240 hour (i.e. 10 day) period. While longer backward-trajectories can lead to greater
121 uncertainty, the general trends remain valuable and 10 days is within a time length commonly studied in past work
122 that utilized HYSPLIT backward-trajectory modeling (Bertschi and Jaffe, 2005; Córdoba-Jabonero et al., 2018;
123 Creamean et al., 2013; Huang et al., 2010; Smith et al., 2013). A new backward-trajectory was simulated for air parcels
124 arriving every 3 hours at the YCFS, at a final elevation of 10 m above surface level. We combined all trajectories
125 simulated during each event observed at the YCFS and the reported North American fires during the period of interest
126 into collective maps using ArcGIS.

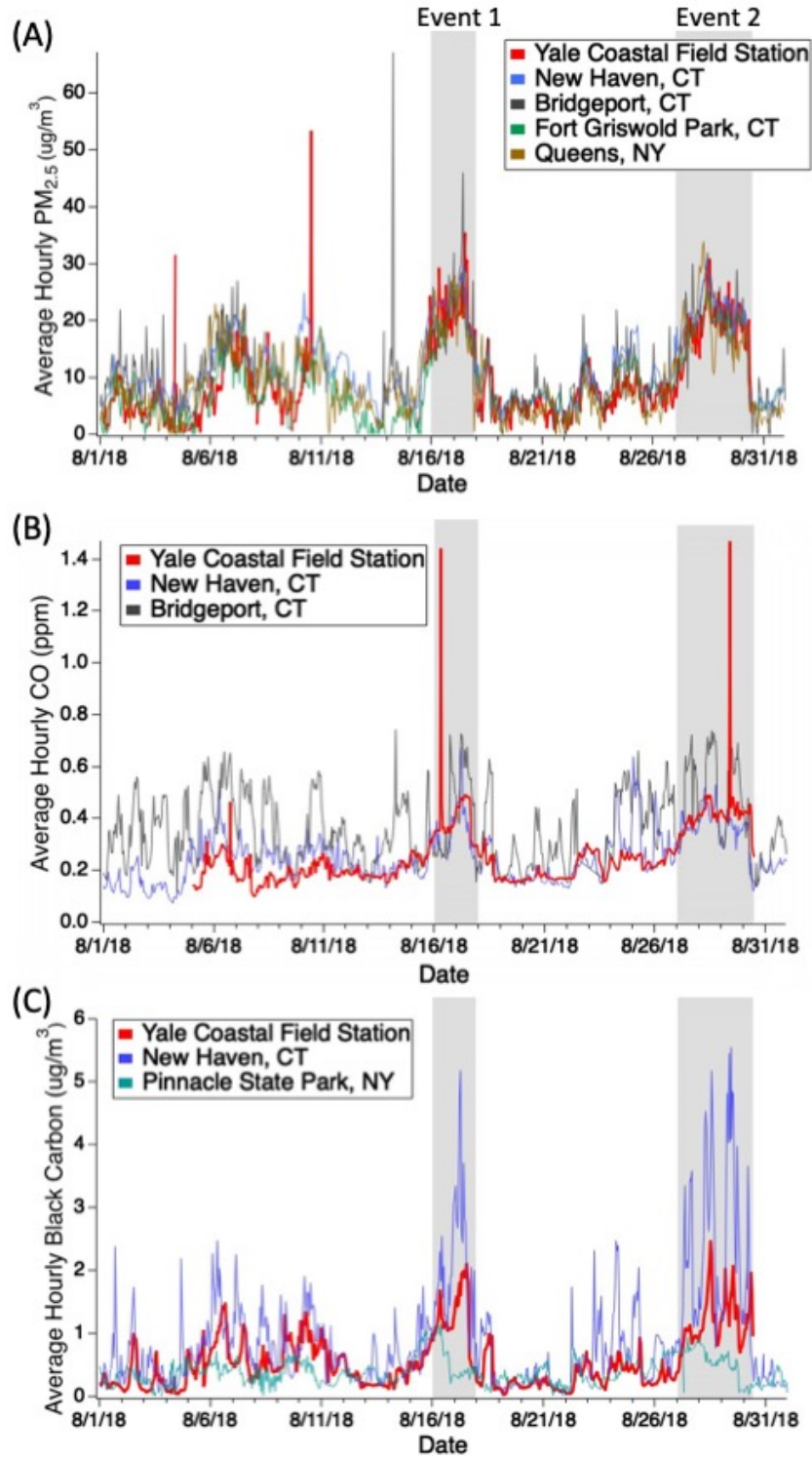
127 **3 Results and Discussion**

128 **3.1 Elevated PM_{2.5}, BC, and CO at the Yale Coastal Field Station and Other Regional Sites**

129 Two main events in August (August 16th-17th and 27th-29th) caused regional concentrations of PM_{2.5}, BC, and CO to
130 all significantly increase for approximately two- and three-day periods, respectively. Figure 2 shows the
131 concentrations measured at the YCFS compared to concentrations measured at nearby sites. The pollution events are
132 multi-day enhancements that are significantly elevated from typical baseline concentrations with some short-term
133 variability in the hourly data observed at only a single site, and thus attributed to local emissions. PM_{2.5} concentrations
134 show strong agreement between different field sites in CT and NY, especially during the two events, confirming that
135 the concentration enhancements were caused by regional changes and not just local sources. Regional BC
136 concentrations show general agreement across the sites with BC data, as well as apparent diurnal patterns at the urban

137 New Haven site, likely from local emissions. However, daily baseline concentrations from the New Haven site are in
138 good agreement with the YCFS site up the coast. The Pinnacle Park site, 300+ km west in upstate New York, is
139 affected by the initial arrival of smoke plumes, but BC concentrations decrease sooner than at the YCFS or New
140 Haven, CT site, which is consistent with the eastward movement of the plumes in the satellite imagery (Figures 3 and
141 4) and backward-trajectories (Figures 5 and 6). CO concentrations have clear multi-day increases at all three field sites
142 during the two identified pollution events. The two urban sites, especially Bridgeport, CT, have greater diurnal changes
143 in CO, potentially caused by local sources (e.g. gasoline-powered motor vehicles), while the YCFS site is generally
144 less affected by local urban emissions.

145
146 Some smaller pollutant enhancements are observed earlier in August (August 6th-7th and August 10th). However, these
147 events have overall lower concentrations than the two events identified on August 16th-17th and August 27th-29th, and
148 satellite smoke maps show minimal smoke influence in the NYC region, with the exception of August 6th (Figure S2).
149 Thus, they were not included in the primary analysis. However, it should be noted that August 5th, 6th, 7th, and 10th
150 were all days where New York State issued an Air Quality Health Alert, primarily for high ozone (New York
151 Department of Environmental Conservation, 2018).



152 Figure 2: Concentrations of PM_{2.5} (panel A), CO (panel B), and BC (panel C) measured at the YCFS over the month of
 153 August, 2018. Grey areas represent the two event periods identified as pollution spikes potentially caused by biomass
 154 burning smoke transport (August 16th-17th and August 27th-29th). These events all show simultaneous increases in PM_{2.5},
 155 CO, and BC across all field sites, well above baseline concentrations. Meteorological dynamics at Pinnacle State Park, NY
 156 (300+ km west) appear to be significantly different and lead to different absolute concentrations and earlier event
 157 dissipation compared to the other sites to the east. Note that the two outlier spikes in CO at the YCFS (panel B) are not

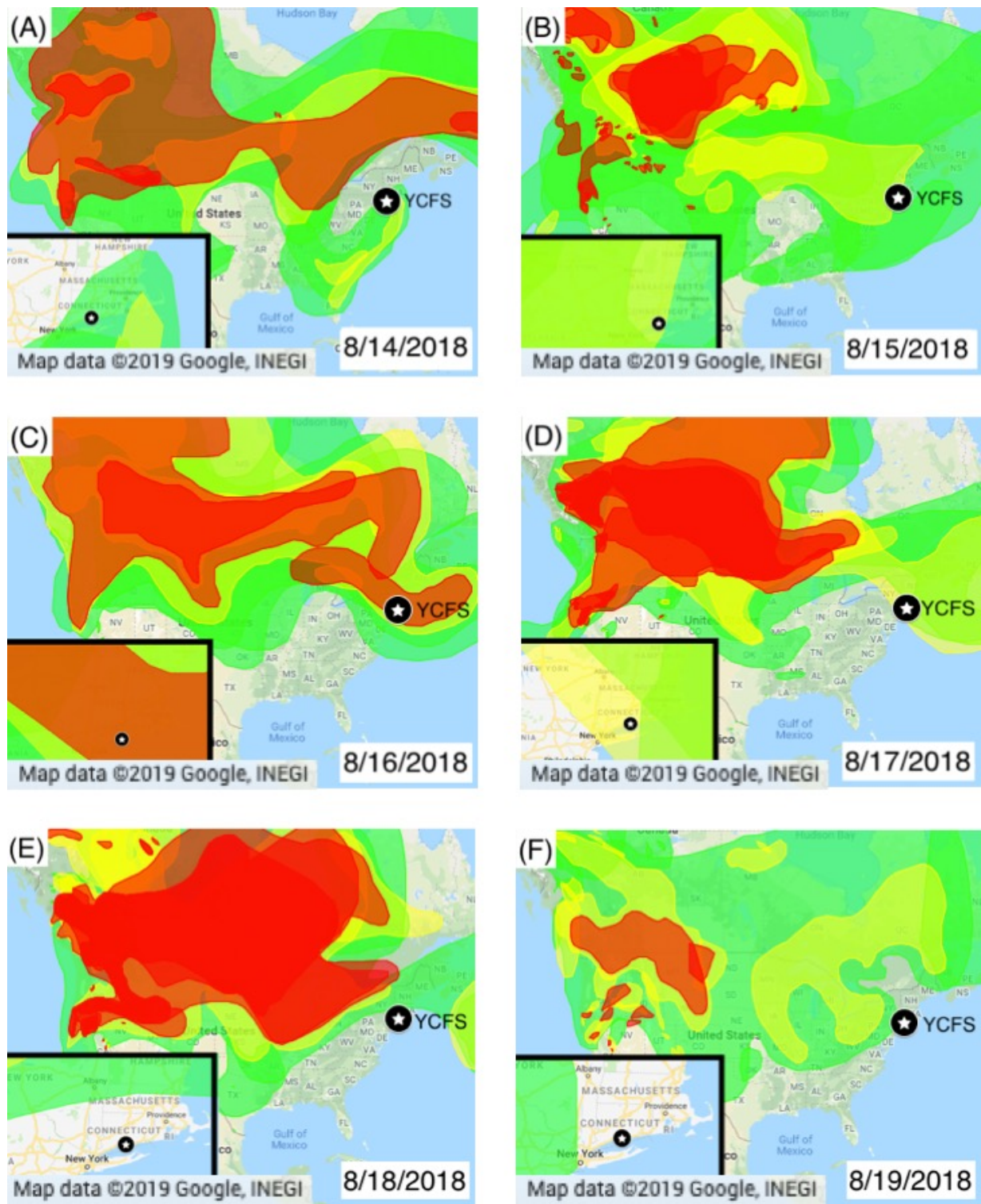
158 ascribed to long-distance transport and are likely due to a hyper-local source near the site (e.g. vehicle, other engine) that
159 caused a brief spike above background levels, evidenced by concurrent NO_x spikes (NO_x is not discussed further in this
160 analysis).

161 3.2 Satellite Imagery: NOAA Smoke Maps

162 NOAA Smoke Maps confirm the presence of smoke over the Long Island Sound area during the regional pollution
163 events with simultaneous enhancements in surface-level concentrations of PM_{2.5}, BC, and CO (Figure 2). This satellite
164 imagery provides evidence that the transport of smoke from biomass burning may have impacted surface-level air
165 quality during the two pollution events. The daily NOAA Smoke Maps in Figures 3-4 show vertically-integrated
166 smoke density before, during, and after these events. Figure 3 shows the arrival of an aloft smoke plume with the total
167 column smoke density peaking at YCFS on August 16th and remaining until the 17th, consistent with the surface-level
168 pollution event on the 16th and 17th (Figure 2). The sharp decrease in surface-level concentrations on the 18th is
169 consistent with the departure of the plume in the satellite imagery (Figure 3E). During the second surface-level
170 pollution event at the end of August, smoke was observed in the region, although less dense than in mid-August.
171 Figure 4 shows a plume lingering over the NYC and CT region from August 27th-29th until the morning of the 30th,
172 which is consistent with surface-level data. No smoke plumes are observed in the area on August 31st (Figure 4F),
173 which is consistent with low surface-level concentrations (Figure 2).

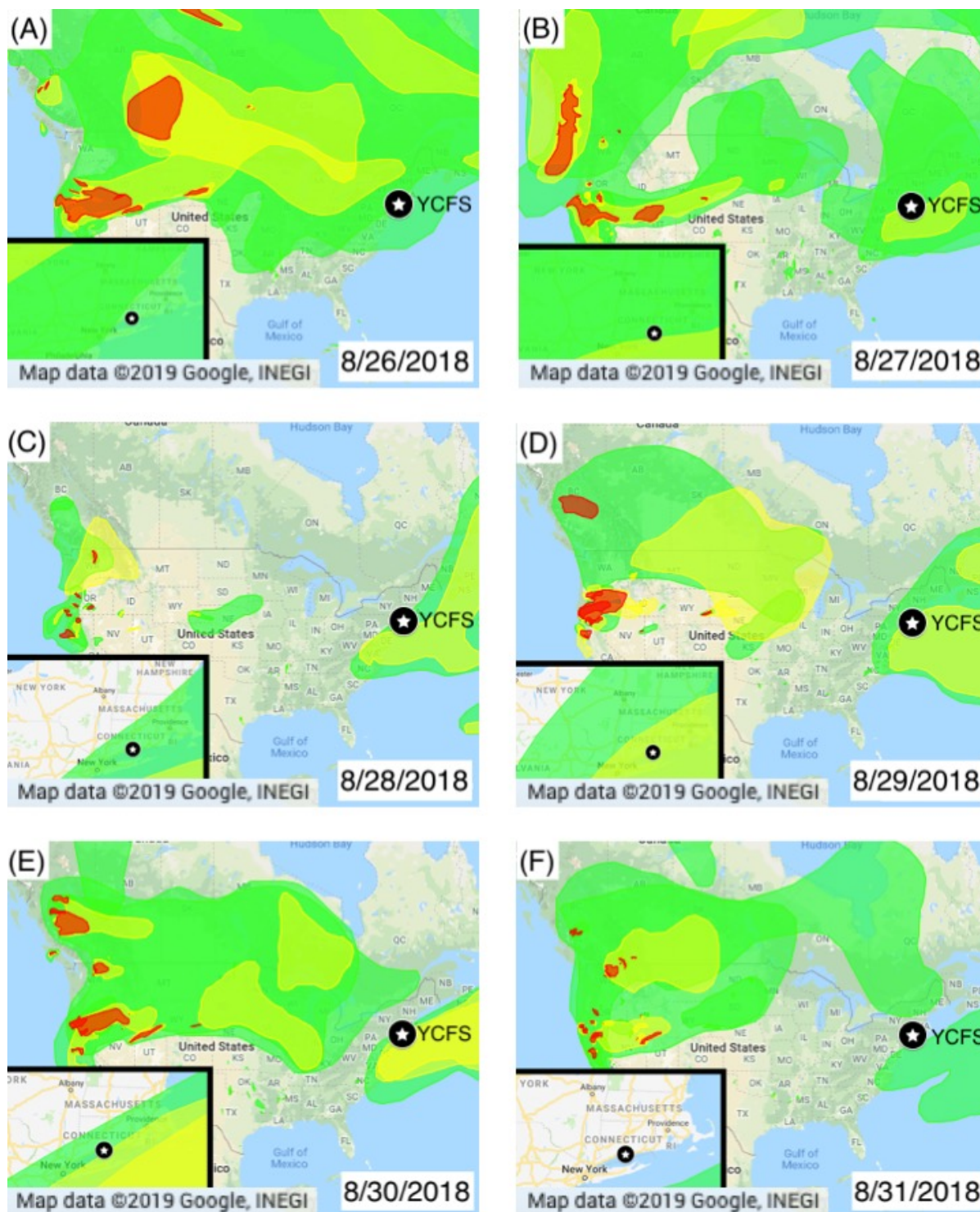
174
175 While the satellite imagery lacks vertical distribution data, the presence of smoke in the region during the same periods
176 when surface-level concentrations increase supports the hypothesis that smoke from aloft was near the surface or
177 available for transport to the surface, and led to the increase in concentrations of PM_{2.5}, BC, and CO at the YCFS and
178 other regional sites. However, the vertically-integrated column measurements represented by the smoke maps are not
179 a perfect prediction of surface-level influence, as shown in the days prior to the actual events (i.e. August 14th-15th,
180 and August 26th). On August 14th-15th leading up to the first event, there are lower levels of smoke aloft over the region
181 that are visible in the satellite imagery (Figure 3A, 3B). On August 26th, leading up to the second event, there is again
182 a low density of smoke over the region (Figure 4A). However, the presence of smoke visible in satellite imagery on
183 days when the surface measurements do not show an increase in air pollutants is not in conflict with surface-level
184 results since it may have been exclusively at higher altitudes. On the days prior to the surface-level events when there
185 is smoke observed aloft in satellite data, it is possible that it had not yet been transported down to the surface sites at

186 the YCFS and others in the region, which is further explored using vertical-resolved backward-trajectories at higher
187 time resolution.



188
189 **Figure 3. Smoke Maps (NOAA) based on satellite imagery for total column measurements for August 14th-19th, 2018: before**
190 **(panels A-B), during (panels C-D), and after (panels E-F) the first surface-level pollution event. The YCFS is indicated by**

191 a star. A new smoke plume begins to arrive aloft on the 15th before the surface-level pollution event on the 16th and 17th with
 192 the aloft total column smoke density peaking on the 16th. The decrease in panels E-F is consistent with the sharp decrease
 193 in surface-level concentrations on the 18th. Colors indicate the intensity of the smoke plume, with red being the most dense,
 194 yellow intermediate, and green the least dense. Insets provide a magnified view of the YCFS site.



195 Figure 4: Smoke Maps (NOAA) based on satellite imagery for total column measurements for August 26th-31st, 2018: before
 196 (panel A), during (panels B-E), and after (panel F) the second surface-level pollution event. The YCFS is indicated by a

197 star. The satellite imagery shows a plume lingering over the region during the period of the surface-level event that spanned
198 from August 27th -29th and continued into the morning of the 30th, which is reflected in the satellite imagery. The absence
199 of smoke aloft in panel F is consistent with low surface-level concentrations. Colors indicate the intensity of the smoke
200 plume, with red being the most dense, yellow intermediate, and green the least dense. Insets provide a magnified view of
201 the YCFS site.

202 3.3 HYSPLIT Backward-Trajectory Model Results

203 Air parcels originating at surface level in areas with wildfires or controlled burns, or passing aloft over regions where
204 wildfires were burning, are likely to pick up aerosols and trace gases associated with biomass burning. Here, we use
205 NOAA HYSPLIT air parcel backward-trajectory models to provide additional information on the horizontally- and
206 vertically-resolved transport pathways as a function of time of day and potential sources that influenced the observed
207 surface-level pollution events in the NYC metropolitan area (Figures 5-6).

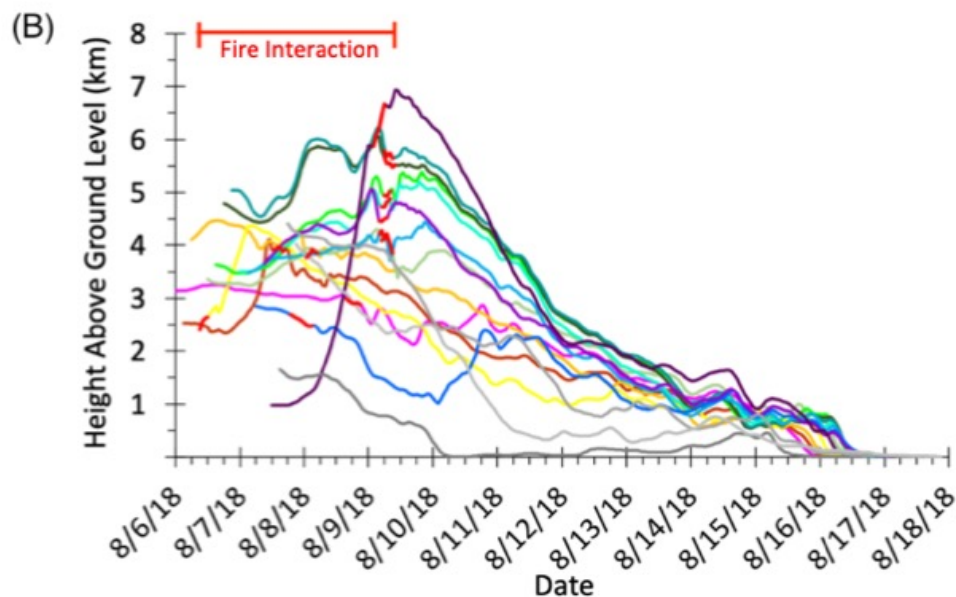
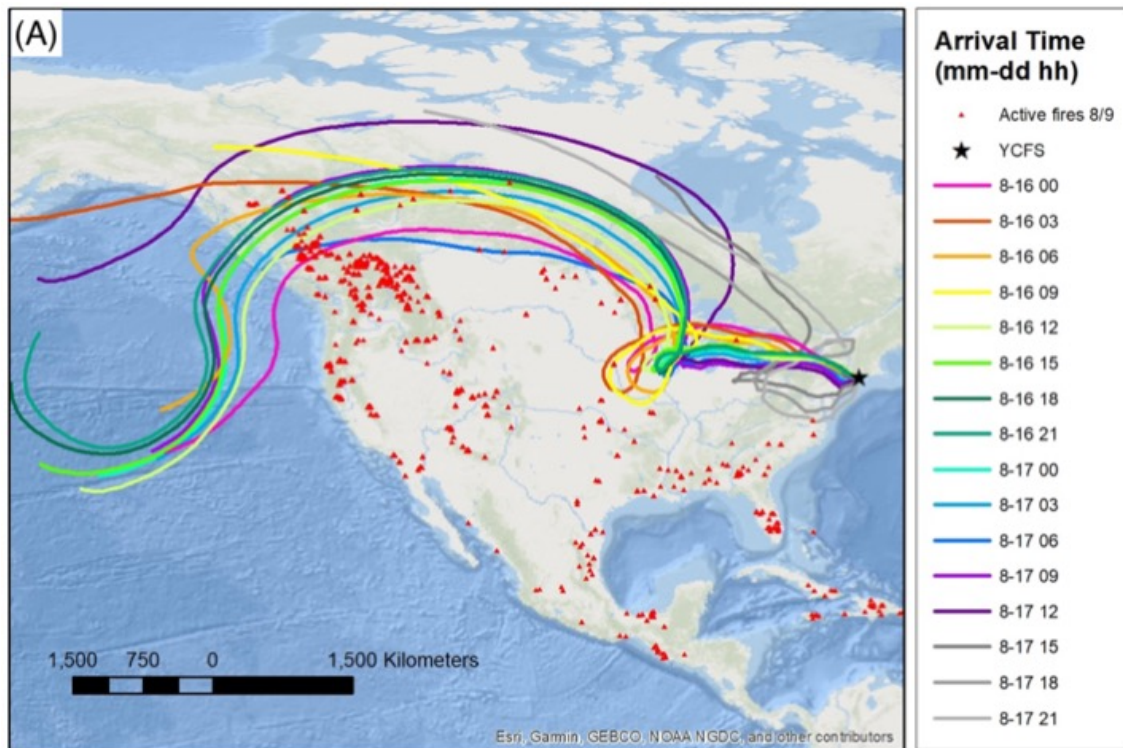
208
209 The backward trajectories for air parcels arriving during the first event (August 16th-17th) show very similar paths
210 passing over the central coast of western Canada (Figure 5), where NOAA's records of fire locations indicate the
211 presence of wildfires in this region during the air parcels' transit. On August 16th, the air parcels' backward-trajectory
212 through Canada and then the northern part of the United States demonstrates that the air parcels passed through an
213 area with numerous active wildfires and descended from aloft to surface-level in the NYC region on August 16th. On
214 August 17th, arriving air parcels follow a similar trajectory to the previous day until later in the day (i.e. 15:00 onward)
215 when air masses did not pass over the North American West Coast within the prior ten days, but stayed in the eastern
216 half of the United States and Canada in areas without reported fires (Figure 5B). This change in transport pathways
217 corresponds with a sharp drop in concentrations of pollutants measured at the YCFS observed at the end of August
218 17th (Figure 2); as wind patterns shifted at the end of August 17th, cleaner air parcels that had not passed through
219 wildfire regions were transported to the YCFS (Figure 5; greyed out), and thus concentrations of associated pollutants
220 dropped. These trajectories re-affirm that the spike in pollutant concentrations measured at the YCFS may have
221 originated from western North American fires for the first event. It is important to note that while most of the
222 backward-trajectories that passed through active fire regions did not pass within 2,000 meters of the surface (Figure
223 5B), emissions in forest fire plumes rise due to the heat of combustion and have been shown to commonly reach
224 heights 2,000-7,000 m above ground level (Colarco et al., 2004; Labonne et al., 2007).

225

226 For the air pollution event occurring on August 27th, 28th, and 29th, backward-trajectory modeling shows the majority
227 of air parcels originated around the Great Lakes region 10 days prior, then circulated in the southeastern U.S. before
228 arriving to the YCFS. While a few trajectories originate on the West Coast, the majority do not pass through the region
229 during the 10 day period. However, these air parcels pass over the southeastern U.S. near surface level (~1500 m and
230 below) where active fires were reported 4-5 days prior to the observed pollution event in the metropolitan NYC region
231 (Figure 6B). This demonstrates the potential role of biomass burning in the southeastern U.S. for air quality in the
232 NYC region and northeast U.S. as well. Many of these fires are likely not wildfires, but other biomass burning events
233 such as intentional crop fires (McCarty et al., 2007). Backward-trajectories for August 27th (the start of the second
234 event) show a similar southeastern circulation pattern as August 28th and 29th (Figure S3). The last 2 trajectories on
235 the 29th do not encounter reported fires (Figure 6; greyed out), which is shortly before the dissipation in concentration
236 at the surface site in the early morning on 8/30 (Figure 2).

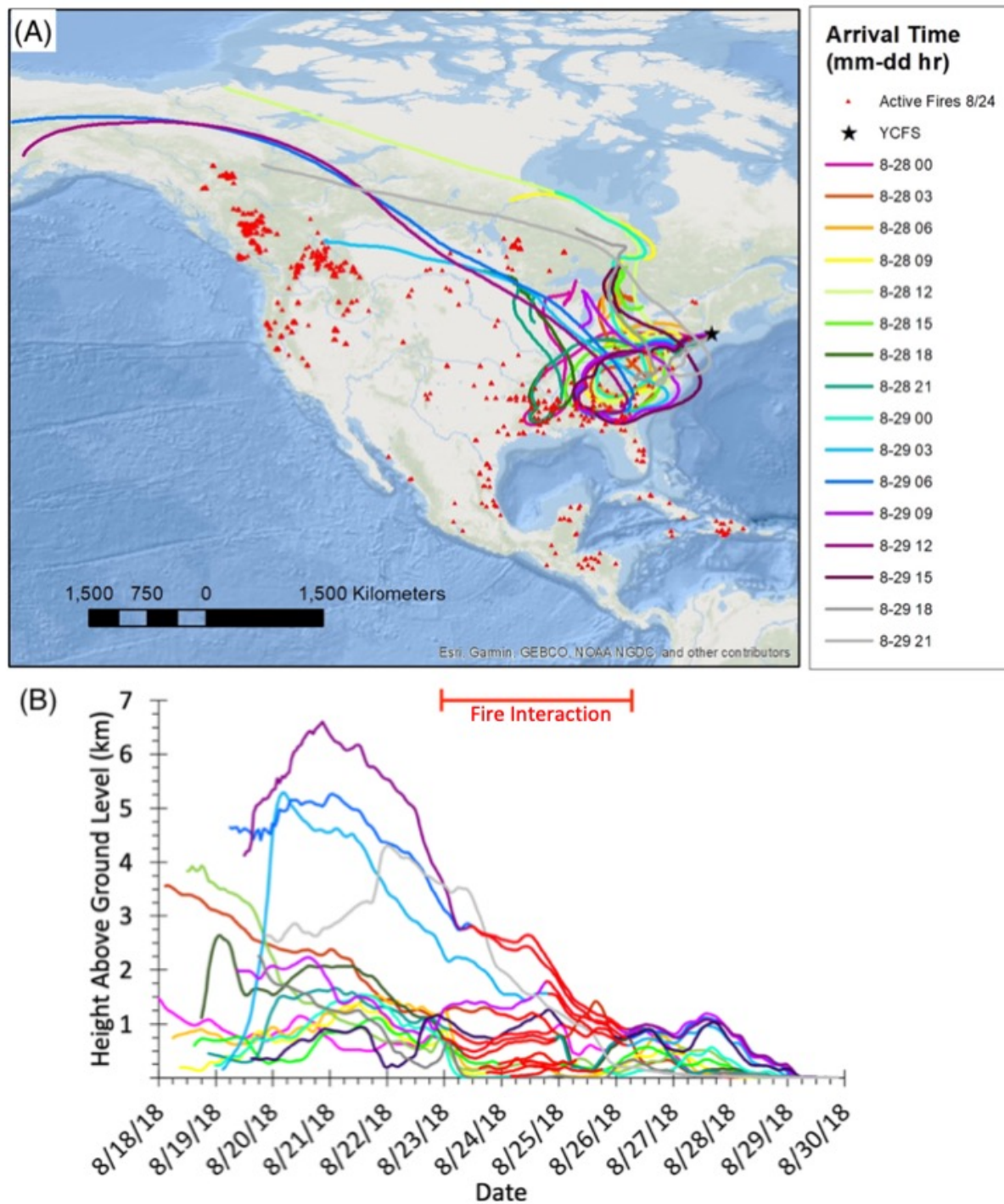
237 While satellite smoke maps (Figures 3-4) show the spatial distribution of (vertically-integrated) smoke across
238 the U.S. during these 2 events, backward trajectories provide more specific evidence that the air parcels observed at
239 the ground-level YCFS site previously passed over active fires and mixed with biomass burning emissions (e.g. BC,
240 CO). The fact that smoke is observed via satellite outputs over the YCFS and the NYC metropolitan area during the
241 same time periods as the ground-level events discussed here, in combination with the fact that that the backward
242 trajectories passed over reported fires (at altitudes where it was reasonable to expect the rising concentrated smoke
243 plumes), provides three different pieces of evidence that long-distance transport of biomass burning emissions
244 impacted air quality in the NYC metropolitan area. In contrast, on many non-event days NOAA Smoke Maps do not
245 show plumes in the YCFS region and backward-trajectories do not show significant interactions with fire locations
246 (examples in Figures 3-4, S4-S7).

247



248

249 Figure 5: NOAA HYSPLIT Backward-trajectory model results for air parcels arriving on August 16th and 17th, 2018 to
 250 surface-level YCFS site. Each line represents the backward-trajectory for an air parcel arriving every three hours
 251 throughout the course of the day. The location of fires on August 9th (when most trajectories intersect the wildfire zone on
 252 the West Coast) is depicted with red triangles (from NOAA HMS fire maps). The top map (A) shows the full 10-day
 253 trajectory and the bottom figure (B) shows the vertical height of each air parcel along its trajectory as well as the times
 254 where it may have intercepted wildfire smoke plumes (highlighted in red on each individual trace, and bracketed above).
 255 The last three trajectories on 8/17 have no major fire interaction, and have thus been colored grey.



256

257 Figure 6: NOAA HYSPLIT Backward-trajectory model results for air parcels arriving on August 28th and 29th, 2018 to
 258 surface-level YCFS site. Each color represents the backward-trajectory for an air parcel arriving every three hours
 259 throughout the course of the day. The location of fires on August 24th (when most trajectories intersect the fire zone in the
 260 southeast U.S.) is depicted with red triangles (from NOAA HMS fire maps). The top map (A) shows the full 10-day
 261 trajectory and the bottom graph (B) shows the vertical height of each air parcel along its trajectory as well as the time
 262 where it may have intercepted fire smoke plumes (highlighted in red on each individual trace). The last two trajectories on
 263 8-29 have no major fire interaction, and have thus been colored grey.

264 4 Conclusions

265 This study provides three pieces of evidence for the potential influence of long-distance transport of emissions from
266 wildfires and other biomass burning on air quality in metropolitan NYC and the northeastern U.S. Together, surface-
267 level measurements made at multiple regional sites, satellite smoke plume imagery, and air parcel backward-trajectory
268 model results indicate that biomass burning smoke was transported to the metropolitan NYC area during two separate
269 events in August leading to elevated levels of PM_{2.5} and BC across the region. First, prolonged regional concentration
270 enhancements in tracers associated with biomass burning—PM_{2.5}, BC, and CO—indicates the potential influence of
271 biomass burning smoke on August 16th-17th and August 27th-29th. Second, NOAA Smoke Maps confirm the arrival
272 and presence of smoke plumes over the Long Island Sound YCFS region on all five days of interest, and their absence
273 after the events. Finally, backward-trajectory models provide additional information on the origin of air parcels and
274 the associated pollutants. Air parcels from August 16th and 17th passed over western Canada, whereas air parcels
275 arriving on August 28th and 29th passed over the southeastern U.S. The sets of trajectories during both events passed
276 over regions with numerous active fires, including wildfires in western Canada, and most likely controlled agricultural
277 burning in the southeast U.S. Regardless of the cause of the fire, these results show that fires in multiple places in
278 North America can impact air quality in metropolitan NYC, in Connecticut, and more broadly, in the northeastern
279 U.S.

280
281 This work, in conjunction with previous studies on the long-distance transport of biomass burning pollutants to other
282 locations (Colarco et al., 2004; Cottle et al., 2014; Dreessen et al., 2016; Jung et al., 2016), reinforces the growing
283 need to understand the long-range influence of wildfires. Increased understanding of long-distance transport is critical
284 for predicting and managing air quality health risks in smoke-impacted areas. During both observed events (Figure
285 2), New York State issued air quality health advisories in New York City Metro and Long Island specifically for ozone
286 (on August 16th, 28th, and 29th) (New York Department of Environmental Conservation, 2018), though the implications
287 of the transported emissions for ozone production are not directly evaluated here. This long-distance transport process
288 is also important since wildfire PM_{2.5} has been specifically shown to have significant health effects with respiratory
289 effects that possibly exceed those of other PM_{2.5} sources, and multi-day wildfire smoke events have even been shown
290 to have short-term health effects on susceptible populations (statistically-significant effects at concentrations >37 µg
291 m⁻³) (Liu et al., 2015; Liu et al., 2017). As climate change continues to impact the likelihood, prevalence, and intensity

292 of wildfires across the U.S. and Canada, air quality scientists and policy makers must pay increasing attention to the
293 influence that these emissions have on air pollution issues, not only on a local scale but nationally and internationally.
294 This is critical as increased emissions throughout a prolonged fire season, when coupled with common meteorological
295 transport, can lead to enhanced background concentrations of primary PM_{2.5} (including BC) and reactive precursors
296 to SOA and ozone (Akagi et al., 2011; Urbanski et al., 2008). In all, these two observed events in the NYC area in
297 August 2018 are examples that demonstrate the role of long-distance transport of biomass burning emissions as
298 important contributors to the evolving air quality challenges facing metro NYC and similar urban areas as local
299 emissions from controllable sources are further reduced (e.g. Khare & Gentner, 2018; NYC Dept. Health, 2018) and
300 wildfires become increasingly frequent.

301 **Author Contributions**

302 H.M.R., J.C.D., and D.R.G. designed the study and led analysis. J.C.D. managed instruments and collected data at the
303 YCFS. H.M.R. analysed data and compiled modeling results and satellite imagery. H.M.R. and D.R.G. wrote the paper
304 and all authors contributed to refining the manuscript.

305 **Competing Interests**

306 The authors declare that they have no conflicts of interest.

307 **Data availability**

308 Data are available upon request to the corresponding author and are in their respective public repositories (LISTOS
309 archive [<https://www-air.larc.nasa.gov/missions/listos/index.html>], EPA Air Quality System
310 [<https://www.epa.gov/aqs>], and NOAA Hazard Mapping System Fire and Smoke Products
311 [<https://www.ospo.noaa.gov/Products/land/hms.html>]).

312 **Acknowledgements**

313 We acknowledge the support of the Yale Department of Chemical and Environmental Engineering undergraduate
314 research funding, the Yale Natural Lands Fund, the Peabody Museum, and the U.S. EPA. This publication was
315 developed under Assistance Agreement No. RD835871 awarded by the U.S. Environmental Protection Agency to
316 Yale University. It has not been formally reviewed by EPA. The views expressed in this document are solely those of
317 the authors and do not necessarily reflect those of the Agency. EPA does not endorse any products or commercial
318 services mentioned in this publication. Thank you as well to Lukas Valin (EPA), Pete Babich (CT DEEP), and David
319 Wheeler and Dirk Felton (NYS DEC and SUNY-ASRC) for instrumentation at the YCFS and data from other sites
320 including Queens and Pinnacle State Park; Rich Boardman, Tim White, and David Skelly (Yale/Peabody), and Ethan
321 Weed and Amir Bond (Peabody EVolutions Interns) for their help establishing the YCFS measurement site; and Paul
322 Miller (NESCAUM) for organizing the LISTOS campaign. The authors gratefully acknowledge the NOAA Air
323 Resources Laboratory (ARL) for the provision of the HYSPLIT transport and dispersion model used in this
324 publication.

325 **References**

326 Abatzoglou, J. T. and Williams, A. P.: Impact of anthropogenic climate change on wildfire across western US forests.,
327 Proc. Natl. Acad. Sci. U. S. A., 113(42), 11770–11775, doi:10.1073/pnas.1607171113, 2016.

328

329 Akagi, S. K., Yokelson, R. J., Wiedinmyer, C., Alvarado, M. J., Reid, J. S., Karl, T., Crounse, J. D. and Wennberg, P.
330 O.: Emission factors for open and domestic biomass burning for use in atmospheric models, Atmos. Chem. Phys,
331 11(9), 4039–4072, doi:10.5194/acp-11-4039-2011, 2011.

332

333 Barbero, R., Abatzoglou, J. T., Larkin, N. K., Kolden, C. A. and Stocks, B.: Climate change presents increased
334 potential for very large fires in the contiguous United States, Int. J. Wildl. Fire, 24(7), 892-899, doi:10.1071/WF15083,
335 2015.

336

337 Barnaba, F., Angelini, F., Curci, G. and Gobbi, G. P.: An important fingerprint of wildfires on the European aerosol
338 load, *Atmos. Chem. Phys.*, 11(20), 10487–10501, doi:10.5194/acp-11-10487-2011, 2011.

339

340 Bertschi, I. T. and Jaffe, D. A.: Long-range transport of ozone, carbon monoxide, and aerosols to the NE Pacific
341 troposphere during the summer of 2003: Observations of smoke plumes from Asian boreal fires, *J. Geophys. Res.*,
342 110(D5), doi:10.1029/2004JD005135, 2005.

343

344 Brook, R. D., Franklin, B., Cascio, W., Hong, Y., Howard, G., Lipsett, M., Luepker, R., Mittleman, M., Samet, J.,
345 Smith, S. C. and Tager, I.: Air pollution and cardiovascular disease: a statement for healthcare professionals from the
346 American Heart Association, *Circulation*, 109(21), 2655–2671, doi:10.1161/01.CIR.0000128587.30041.C8, 2004.

347

348 Burgos, M. A., Mateos, D., Cachorro, V. E., Toledano, C., de Frutos, A. M., Calle, A., Herguedas, A. and Marcos, J.
349 L.: An analysis of high fine aerosol loading episodes in north-central Spain in the summer 2013 - Impact of Canadian
350 biomass burning episode and local emissions, *Atmos. Environ.*, 184, 191–202, doi:10.1016/j.atmosenv.2018.04.024,
351 2018.

352

353 Calvo, A. I., Alves, C., Castro, A., Pont, V., Vicente, A. M. and Fraile, R.: Research on aerosol sources and chemical
354 composition: Past, current and emerging issues, *Atmos. Res.*, 120, 1–28, doi:10.1016/J.ATMOSRES.2012.09.021,
355 2013.

356

357 Colarco, P. R., Schoeberl, M. R., Doddridge, B. G., Marufu, L. T., Torres, O. and Welton, E. J.: Transport of smoke
358 from Canadian forest fires to the surface near Washington, D.C.: Injection height, entrainment, and optical properties,
359 *J. Geophys. Res. Atmos.*, 109(D6), n/a-n/a, doi:10.1029/2003JD004248, 2004.

360

361 Córdoba-Jabonero, C., Sicard, M., Ansmann, A., Del Águila, A. and Baars, H.: Separation of the optical and mass
362 features of particle components in different aerosol mixtures by using POLIPHON retrievals in synergy with
363 continuous polarized Micro-Pulse Lidar (P-MPL) measurements, *Atmos. Meas. Tech.*, 11(8), 4775–4795,
364 doi:10.5194/amt-11-4775-2018, 2018.

365
366 Cottle, P., Strawbridge, K. and McKendry, I.: Long-range transport of Siberian wildfire smoke to British Columbia:
367 Lidar observations and air quality impacts, *Atmos. Environ.*, 90, 71–77, doi:10.1016/j.atmosenv.2014.03.005, 2014.
368
369 Creamean, J. M., Suski, K. J., Rosenfeld, D., Cazorla, A., DeMott, P. J., Sullivan, R. C., White, A. B., Ralph, F. M.,
370 Minnis, P., Comstock, J. M., Tomlinson, J. M. and Prather, K. A.: Dust and Biological Aerosols from the Sahara and
371 Asia Influence Precipitation in the Western U.S., *Science*, 339(6127), 1572–1578, doi:10.1126/science.1227279,
372 2013.
373
374 Cubison, M. J., Ortega, A. M., Hayes, P. L., Farmer, D. K., Day, D., Lechner, M. J., Brune, W. H., Apel, E., Diskin,
375 G. S., Fisher, J. A., Fuelberg, H. E. Hecobian, A., Knapp, D. J., Mikoviny, T., Riemer, D., Sachse, G. W., Sessions,
376 W., Weber, R. J., Weinheimer, A. J., Wisthaler, A., and Jimenez, J. L.: Effects of aging on organic aerosol from open
377 biomass burning smoke in aircraft and laboratory studies, *Atmos. Chem. Phys.*, 11, 12049-12064, doi: :10.5194/acp-
378 11-12049-2011, 2011.
379
380 Diapouli, E., Popovicheva, O., Kistler, M., Vratolis, S., Persiantseva, N., Timofeev, M., Kasper-Giebl, A. and
381 Eleftheriadis, K.: Physicochemical characterization of aged biomass burning aerosol after long-range transport to
382 Greece from large scale wildfires in Russia and surrounding regions, Summer 2010, *Atmos. Environ.*, 96, 393–404,
383 doi:10.1016/j.atmosenv.2014.07.055, 2014.
384
385 Dockery, D. W., Pope, C. A., Xu, X., Spengler, J. D., Ware, J. H., Fay, M. E., Ferris, B. G. and Speizer, F. E.: An
386 Association between air pollution and mortality in six U.S. cities, *N. Engl. J. Med.*, 329(24), 1753–1759,
387 doi:10.1056/NEJM199312093292401, 1993.
388
389 Dreessen, J., Sullivan, J. and Delgado, R.: Observations and impacts of transported Canadian wildfire smoke on ozone
390 and aerosol air quality in the Maryland region on June 9–12, 2015, *J. Air Waste Manage. Assoc.*, 66(9), 842–862,
391 doi:10.1080/10962247.2016.1161674, 2016.
392

393 Forster, C., Wandering, U., Wotawa, G., James, P., Mattis, I., Althausen, D., Simmonds, P., O'Doherty, S., Jennings,
394 S. G., Kleefeld, C., Schneider, J., Trickl, T., Kreipl, S., Jäger, H. and Stohl, A.: Transport of boreal forest fire emissions
395 from Canada to Europe, *J. Geophys. Res. Atmos.*, 106(D19), 22887–22906, doi:10.1029/2001JD900115, 2001.
396

397 Hennigan, C. J., Miracolo, M. A., Engelhart, G. J., May, A. A., Presto, A. A., Lee, T., Sullivan, A. P., McMeeking,
398 G. R., Coe, H., Wold, C. E., Hao, W.-M., Gilman, J. B., Kuster, W. C., de Gouw, J., Schichtel, B. A., Collett Jr., J. L.,
399 Kreidenweis, S. M., and Robinson, A. L.: Chemical and physical transformations of organic aerosol from the photo-
400 oxidation of open biomass burning emissions in an environmental chamber, *Atmos. Chem. Phys.*, 11, 7669–7686, doi:
401 10.5194/acp-11-7669-2011, 2011.
402

403 Huang, L., Gong, S. L., Sharma, S., Lavoué, D. and Jia, C. Q.: A trajectory analysis of atmospheric transport of black
404 carbon aerosols to Canadian high Arctic in winter and spring (1990-2005), *Atmos. Chem. Phys.*, 10(11), 5065–5073,
405 doi:10.5194/acp-10-5065-2010, 2010.
406

407 Jacob, Daniel J.: *Introduction to Atmospheric Chemistry*, Princeton University Press, Princeton, New Jersey, 1999.
408

409 Jung, J., Lyu, Y., Lee, M., Hwang, T., Lee, S. and Oh, S.: Impact of Siberian forest fires on the atmosphere over the
410 Korean Peninsula during summer 2014, *Atmos. Chem. Phys.*, 16(11), 6757–6770, doi:10.5194/acp-16-6757-2016,
411 2016.
412

413 Khare, P. and Gentner, D. R.: Considering the future of anthropogenic gas-phase organic compound emissions and
414 the increasing influence of non-combustion sources on urban air quality, *Atmos. Chem. Phys.*, 18, 5391–5413,
415 <https://doi.org/10.5194/acp-18-5391-2018>, 2018.
416

417 Labonne, M., Bréon, F.-M. and Chevallier, F.: Injection height of biomass burning aerosols as seen from a spaceborne
418 lidar, *Geophys. Res. Lett.*, 34(11), doi:10.1029/2007GL029311, 2007.
419

420 Lewis, K., Arnott, W. P., Moosmüller, H. and Wold, C. E.: Strong spectral variation of biomass smoke light absorption
421 and single scattering albedo observed with a novel dual-wavelength photoacoustic instrument, *J. Geophys. Res.*,
422 113(D16), doi:10.1029/2007JD009699, 2008.

423

424 Liu, J. C., Pereira, G., Uhl, S. A., Bravo, M. A. and Bell, M. L.: A systematic review of the physical health impacts
425 from non-occupational exposure to wildfire smoke, *Environ. Res.*, 136, 120–132,
426 doi:10.1016/J.ENVRES.2014.10.015, 2015.

427

428 Liu, J. C., Wilson, A., Mickley, L. J., Dominici, F., Ebisu, K., Wang, Y., Sulprizio, M. P., Peng, R. D., Yue, X., Son,
429 J. Y., Anderson, G. B., and Bell, M. L.: Wildfire-specific Fine Particulate Matter and Risk of Hospital Admissions in
430 Urban and Rural Counties, *Epidemiology*, 28(1), 77-85, doi:10.1097/EDE.0000000000000556, 2017.

431

432 Martín, M. V., Honrath, R. E., Owen, R. C., Pfister, G., Fialho, P. and Barata, F.: Significant enhancements of nitrogen
433 oxides, black carbon, and ozone in the North Atlantic lower free troposphere resulting from North American boreal
434 wildfires, *J. Geophys. Res. Atmos.*, 111(D23), doi:10.1029/2006JD007530, 2006.

435

436 McCarty, J, Justice, C., Korontzi, S.: Agricultural burning in the Southeastern United States detected by MODIS,
437 *Remote Sensing of Environment*, 108(2), 151-162, doi: 10.1016/j.rse.2006.03.020, 2007.

438

439 New York Department of Environmental Conservation: 2018 Press Releases, available at:
440 <https://www.dec.ny.gov/press/115749.html> (last access: 16 October 2019), 2018.

441

442 New York City Department of Health: The New York City Community Air Survey: Neighborhood Air Quality 2008-
443 2016; New York City, available at: [https://www1.nyc.gov/assets/doh/downloads/pdf/environmental/comm-air-](https://www1.nyc.gov/assets/doh/downloads/pdf/environmental/comm-air-survey-08-16.pdf)
444 [survey-08-16.pdf](https://www1.nyc.gov/assets/doh/downloads/pdf/environmental/comm-air-survey-08-16.pdf) (last access: 4 November 2019), 2018.

445

446 Niemi, J. V., Tervahattu, H., Vehkamäki, H., Martikainen, J., Laakso, L., Kulmala, M., Aarnio, P., Koskentalo, T.,
447 Sillanpää, M. and Makkonen, U.: Characterization of aerosol particle episodes in Finland caused by wildfires in
448 Eastern Europe, *Atmos. Chem. Phys.*, 5(8), 2299–2310, doi:10.5194/acp-5-2299-2005, 2005.

449

450 NOAA: Fire Products Archive, [online] Available from: <https://satepsanone.nesdis.noaa.gov/FIRE/fire.html>
451 (Accessed 20 December 2018), 2018.

452

453 Reid, C. E., Brauer, M., Johnston, F. H., Jerrett, M., Balmes, J. R. and Elliott, C. T.: Critical review of health impacts
454 of wildfire smoke exposure, *Environ. Health Perspect.*, 124(9), 1334-1343, doi:10.1289/EHP.1409277, 2016.

455

456 Smith, D. J., Timonen, H. J., Jaffe, D. A., Griffin, D. W., Birmele, M. N., Perry, K. D., Ward, P. D. and Roberts, M.
457 S.: Intercontinental dispersal of bacteria and archaea by transpacific winds, *Appl. Environ. Microbiol.*, 79(4), 1134–
458 1139, doi:10.1128/AEM.03029-12, 2013.

459

460 Stein, A. F., Draxler, R. R., Rolph, G. D., Stunder, B. J. B., Cohen, M. D., Ngan, F., Stein, A. F., Draxler, R. R., Rolph,
461 G. D., Stunder, B. J. B., Cohen, M. D. and Ngan, F.: NOAA’s HYSPLIT Atmospheric Transport and Dispersion
462 Modeling System, *Bull. Am. Meteorol. Soc.*, 96(12), 2059–2077, doi:10.1175/BAMS-D-14-00110.1, 2015.

463

464 Stohl, A., Forster, C., Eckhardt, S., Spichtinger, N., Huntrieser, H., Heland, J., Schlager, H., Wilhelm, S., Arnold, F.
465 and Cooper, O.: A backward modeling study of intercontinental pollution transport using aircraft measurements, *J.*
466 *Geophys. Res.*, 108(D12), doi:10.1029/2002JD002862, 2003.

467

468 U.S. Census Bureau: American FactFinder - Annual Estimates of the Resident Population: April 1, 2010 to July 1,
469 2017 - United States -- Metropolitan Statistical Area; 2017 Population Estimates, [online] Available from:
470 <https://factfinder.census.gov/faces/tableservices/jsf/pages/productview.xhtml?src=bkmk> (Accessed 5 May 2019),
471 2017.

472

473 Urbanski, S. P., Hao, W. M. and Baker, S.: Chemical composition of wildland fire emissions, *Dev. Environ. Sci.*, 8,
474 79–107, doi:10.1016/S1474-8177(08)00004-1, 2008.

475

476 Vicente, A., Alves, C., Calvo, A. I., Fernandes, A. P., Nunes, T., Monteiro, C., Almeida, S. M. and Pio, C.: Emission
477 factors and detailed chemical composition of smoke particles from the 2010 wildfire season, *Atmos. Environ.*, 71,
478 295–303, doi:10.1016/j.atmosenv.2013.01.062, 2013.

479

480 Ward, D. E. and Hardy, C. C.: Smoke emissions from wildland fires, *Environ. Int.*, 17(2–3), 117–134,
481 doi:10.1016/0160-4120(91)90095-8, 1991.

482

483 Yokelson, R. J., Burling, I. R., Gilman, J. B., Warneke, C., Stockwell, C. E., De Gouw, J., Akagi, S. K., Urbanski, S.
484 P., Veres, P., Roberts, J. M., Kuster, W. C., Reardon, J., Griffith, D. W. T., Johnson, T. J., Hosseini, S., Miller, J. W.,
485 Cocker Iii, D. R., Jung, H. and Weise, D. R.: Coupling field and laboratory measurements to estimate the emission
486 factors of identified and unidentified trace gases for prescribed fires, *Atmos. Chem. Phys*, 13(1), 89–116,
487 doi:10.5194/acp-13-89-2013, 2013.

488